Original Research   *Feature article*

Assessment of the influence on left ventricle by potassium oxonate and hypoxanthine–induced chronic hyperuricemia

Cuiting Lin[1], Qiang Zheng[1], Yongmei Li[1], Ting Wu[1], Jian Luo[1], Yanqing Jiang[1], Qinghua Huang[1], Caixin Yan[1], Leqi Zhang[1], Wei Zhang[1], Hui Liao[1], Yang Yang[1,2] and Jianxin Pang[1]

[1]Guangdong Provincial Key Laboratory of Drug Screening, School of Pharmaceutical Sciences, Southern Medical University, Guangzhou 510515, Guangdong, China; [2]Affiliated Foshan Maternity & Child Healthcare Hospital, Southern Medical University, Foshan 528000, Guangdong, China
Corresponding authors: Jianxin Pang. Email: pjx@smu.edu.cn; Yang Yang. Email: jzyy727@foxmail.com

Impact Statement

Currently, growing evidence has indicated that hyperuricemia (HUA) is an independent factor of left ventricular hypertrophy and diastolic dysfunction. The serum uric acid concentration is highly correlated with the risk of chronic heart disease events and poor prognosis. A valid animal model is important for pathological and pharmacological research. In this study, we used potassium oxonate and hypoxanthine to induce chronic HUA in Kunming mice and observed left ventricular remodeling after eight weeks of treatment. We hope that this article will implicate the validation of this model for future investigations on the mechanisms and therapeutic treatment evaluations of HUA-associated heart injury.

Abstract

Cellular cytoplasmic xanthine oxidase (XO)–mediated uric acid synthesis and extracellular excess uric acid exposure are both causes of cardiomyocytic injury under the condition of hyperuricemia (HUA). Potassium oxonate suppresses uric acid degradation to increase extracellular concentration, while hypoxanthine is the catalytic substrate of XO. We aimed to observe cardiac damage in a chronic HUA mouse model induced by potassium oxonate and hypoxanthine. The mouse model was established by the co-administration of potassium oxonate and hypoxanthine for eight weeks. Then, left ventricular parameters were examined by echocardiographic evaluation, and the heart tissues were harvested for further histopathological analysis. The results showed that plasma uric acid was persistently elevated in the model mice, which demonstrated the stable establishment of chronic HUA. The left ventricular anterior wall was significantly thickened in the model group compared with the blank control group. After the end of modeling, the left ventricular anterior wall thickness of the hyperuricemic mice increased compared with that of blank group. The histological analysis showed and myocardial structure disorganization in the model group compared with the blank control. The above cardiac impairment changes could be attenuated by allopurinol pretreatment. This study systematically assessed cardiac damage in a chronic HUA mouse model. In addition, it provides useful information for future HUA-associated heart injury mechanism investigation and therapeutic treatment evaluation.

Keywords: Hyperuricemia, heart, ventricular remodeling, potassium oxonate, hypoxanthine, uric acid

Introduction

Hyperuricemia (HUA) is the fourth most common basal metabolic disease after hypertension, hyperlipidemia, and hyperglycemia. Currently, most studies have focused on acute injuries caused by HUA, such as acute kidney injury, or gout. Most of the existing HUA animal models were established based on these specific evaluation purposes. In fact, HUA is a chronic disease, and the associated complication assessment in the long term cannot be ignored. Recently, the effect of long-term HUA on cardiovascular diseases has attracted attention. Growing evidence has indicated that HUA is an independent factor for left ventricular hypertrophy as well as diastolic dysfunction,[1,2] and the serum uric acid concentration is highly associated with chronic heart disease incident risk and poor prognosis.[3,4] The 2021 expert consensus for the diagnosis and treatment of HUA highlights the importance of controlling uric acid in patients with cardiovascular diseases.[5]

However, animal models have seldom systematically assessed the changes in cardiac function and pathology under long-term chronic HUA stimulation. Mice and rats are the most commonly used animal models, but unlike humans and great apes, they synthesize the uricase enzyme (UOX) to metabolize uric acid to allantoin.[6,7] This leads to lowering of uric acid after the metabolism and excretion of the HUA

inducer and causes a uric acid deficiency in some organs. Previous research indicated that UOX knockout mice always died before adulthood with serious kidney injury.[8,9] Thus, the current gene-editing method is still rudimentary and not suitable for assessing HUA-associated chronic complications. Both cellular cytoplasmic uric acid production and extracellular uric acid exposure can promote cardiomyocytic injury.[10,11] Given this, the co-administration of two or more chemicals targeting the above-mentioned mechanisms has been reported to help establish a chronic HUA animal model. The reported HUA chemical inducers include potassium oxonate, xanthine, hypoxanthine, yeast, adenine, ethambutol, and fructose. Potassium oxonate is usually applied to mimic human purine metabolism to consume uricase to sustain the uric acid level.[12] Hypoxanthine is the precursor of uric acid and can be catalyzed *in vivo* by XO.[13]

In this study, we used a co-administration method of potassium and hypoxanthine to induce Kunming mice suffering from long-term HUA and systematically assessed the left ventricular functional and pathological changes. Compared with previous publications, we controlled the uric concentration in the range of clinical diagnostic criteria and confirmed other common complications previously reported. This study may contribute to model selection for future research on HUA-associated heart injury protection and intervention.

Materials and methods

Chemical and reagents

0.5% sodium carboxy methyl cellulose (CMC-Na) was prepared with sterile physiological saline as the solvent of HUA chemical inducers. Potassium oxonate (Aladdin Biochemical Technology, Shanghai, China; P137112) and hypoxanthine (Shanghai Macklin Biochemical Co., Ltd, Shanghai, China; H6263) were suspended in 0.5% CMC-Na solvent as the stock with the concentration of 35 and 45 mg/mL, respectively, and homogenized with ultrasound before use. Allopurinol (Sigma-Aldrich, Germany; A8003) was dissolved in saline with the concentration of 1 mg/mL as stock for further use.

Experimental animals

Healthy specific pathogen-free (SPF) Male Kunming (KM) mice, weight 20 ± 2 g, were provided by the Laboratory Animal Center of Southern Medical University (Guangzhou, China). All animal experiments were carried out in accordance with the Institutional Animal Care Committee at the Southern Medical University, and followed the national and animal experimental ethics standards. The animals were fed with common feed for one week in the suitable experimental environment with 12 h of 12 h light/dark cycle rhythm regulation, room temperature (25 ± 1°C), and humidity (50 ± 10%). Thirty-six mice were randomly divided into three groups: blank group, HUA model group, and allopurinol group. Both HUA group and allopurinol group mice received the treatment of daily intraperitoneal injection of potassium oxonate 350 mg/kg and oral gavage of hypoxanthine 450 mg/kg, while blank group with the same amount of solvent. Allopurinol group received 5 mg/kg allopurinol

gavage 1 h prior to modeling, others with saline. All of the mice performed cardiac color ultrasound examination after eight weeks of treatment and were sacrificed subsequently.

Blood samples and biochemical analysis

Blood samples were collected from all animals in heparin anticoagulation tubes, and then centrifuged at 3000 rcf for 10 min at 4°C. The supernatant was isolated and stored at −20°C for biochemical measurements. The uric acid concentration was measured by a QuantiChrom™ Uric Acid Assay Kit (BioAssay Systems, Hayward, CA, USA; DIUA-250). The XO was measured by a XO Activity Assay Kit (Solarbio, Beijing, China; BC1095).

Echocardiography examination

All of the animals received echocardiography examination at the end of the 8th week by an ultra high-frequency and high-resolution small animal ultrasonic imaging system (VEVO 2100, Visual Sonics, Toronto, Canada). Before the ultrasound procedure, the mice were fasted for 8 h, and the hair on the front chest was removed to expose the examination site using an electric hair shaver. Animals were under anesthetic sedation during the ultrasound evaluation; 1.5% pentobarbital (45 mg/kg) was administered via intraperitoneal injection 10 min prior to the procedure. Heat preservation and proper subcutaneous injection for rehydration and resuscitation care were provided. The left ventricular anterior wall (LVAW) and left ventricular posterior wall (LVPW) thickness, and left ventricular internal diameter (LVID) in both the diastolic stage and systolic stage were measured. Cardiac function parameters – such as left ventricular end-diastolic volume (LVEdV), left ventricular end-systolic stage volume (LVEsV), stroke volume (SV), ejection fraction (EF), fraction shortening (FS), and left ventricular mass corrected (LV mass) – were calculated by the system software based on the measurements.

Histopathology

The animals were sacrificed immediately after blood collection. The organs were dissected, photographed, and weighed as soon as possible and then transferred to Eppendorf tubes prefilled with 4% paraformaldehyde. Paraffin-embedded tissue specimens were prepared into 4 μm-thick sections for further hematoxylin–eosin (H&E) and Masson's trichrome staining and assessed by light microscopy.

Statistical analysis

The bar charts were processed by GraphPad Prism 8.0 (GraphPad Software, San Diego, CA, USA) and expressed as mean value $\pm$ standard deviation (SD). Statistical differences between groups were determined by independent two-sample *t*-test. $P < 0.05$ was considered to be statistically significantly (*$P \leqslant 0.05$; **$P \leqslant 0.01$; ***$P \leqslant 0.001$).

Bioinformatics data mining

The gene expression information of GSE84796 was retrieved from the National Center for Biotechnology Information
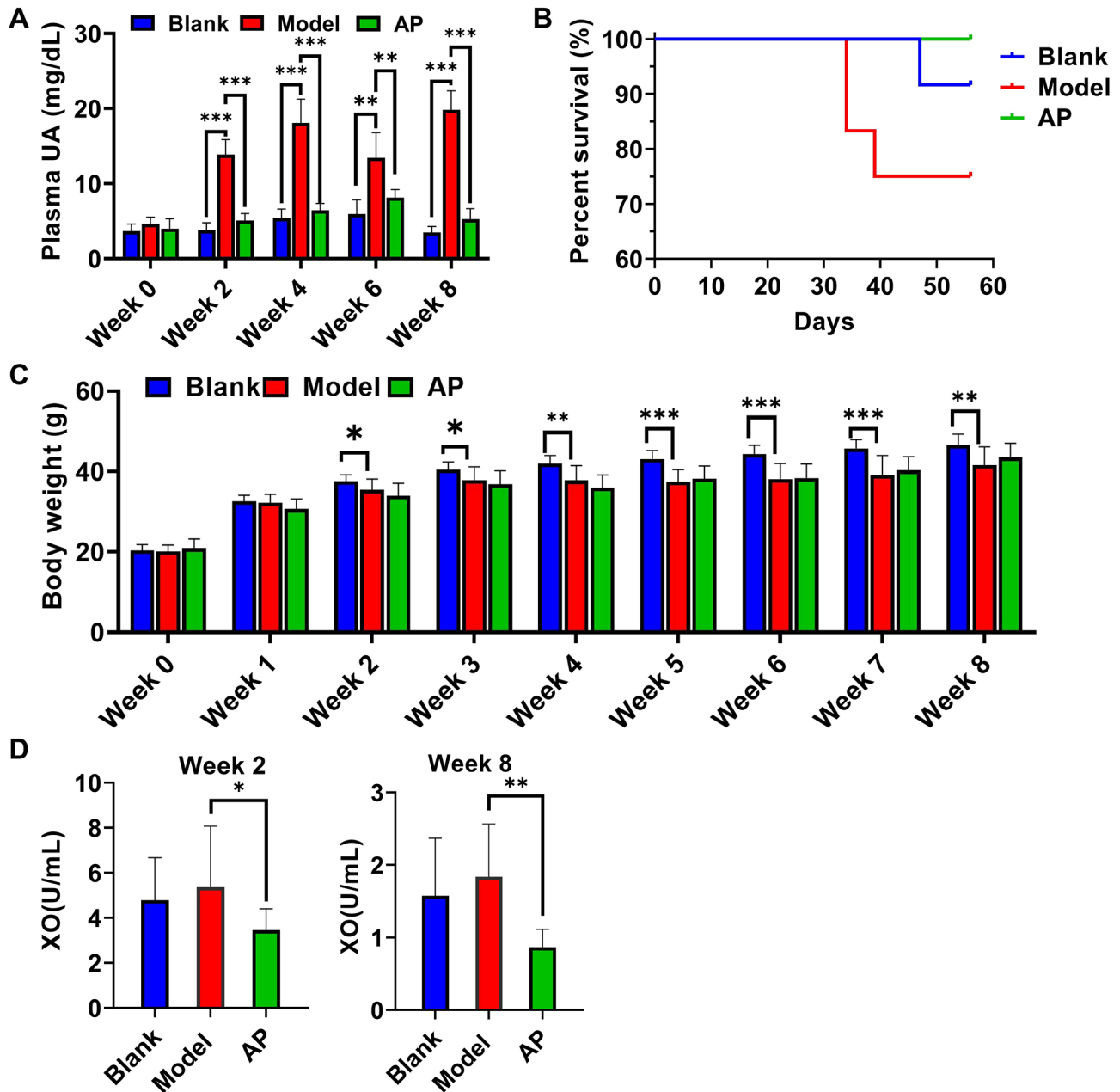
Figure 1. Basic characters throughout eight weeks modeling. (A) plasma uric acid concentration (week 0–4: $n = 6$; week 6: blank $n = 6$, model $n = 4$, AP $n = 6$; week 8: blank $n = 5$, model $n = 5$, AP $n = 6$); (B) survive curve among groups; (C) body weight monitoring (week 0–4: $n = 12$; week 5: blank $n = 12$, model $n = 10$, AP $n = 12$; week 6: blank $n = 12$, model $n = 9$, AP $n = 12$; week 7–8: blank $n = 11$, model $n = 9$, AP $n = 12$); (D) plasma XO concentration (week 2: $n = 12$; week 8: blank $n = 11$, model $n = 9$, AP $n = 12$). Data are presented as mean value $\pm$ SD.
*$P \leqslant 0.05$; **$P \leqslant 0.01$; ***$P \leqslant 0.001$.

(NCBI) Gene Expression Omnibus (GEO) database. The multivariate correlations were visualized using R software with the corrplot package. Correlation parameters and curves were generated using Python software with the seaborn package.

Results

Basic characters description

As expected, during the entire modeling period, the plasma uric acid level in the model group was significantly increased compared with that in the blank group, and it was sensitive to the urate-lowering agent allopurinol (Figure 1(A)). After eight weeks of modeling, 75% of the model mice, 92% of the blank mice, and 100% of the allopurinol mice survived. The starting time of mouse death in the model group was shorter than that in the blank group (Figure 1(B)). The body weight of all groups increased throughout the whole modeling period. However, the body weight gain in the second week was significantly less in the model group than in the blank group, and allopurinol treatment did not significantly improve this parameter (Figure 1(C)). The plasma XO showed increase in model group compare with blank group in both week 2 and week 8, but the differences did not show significance.
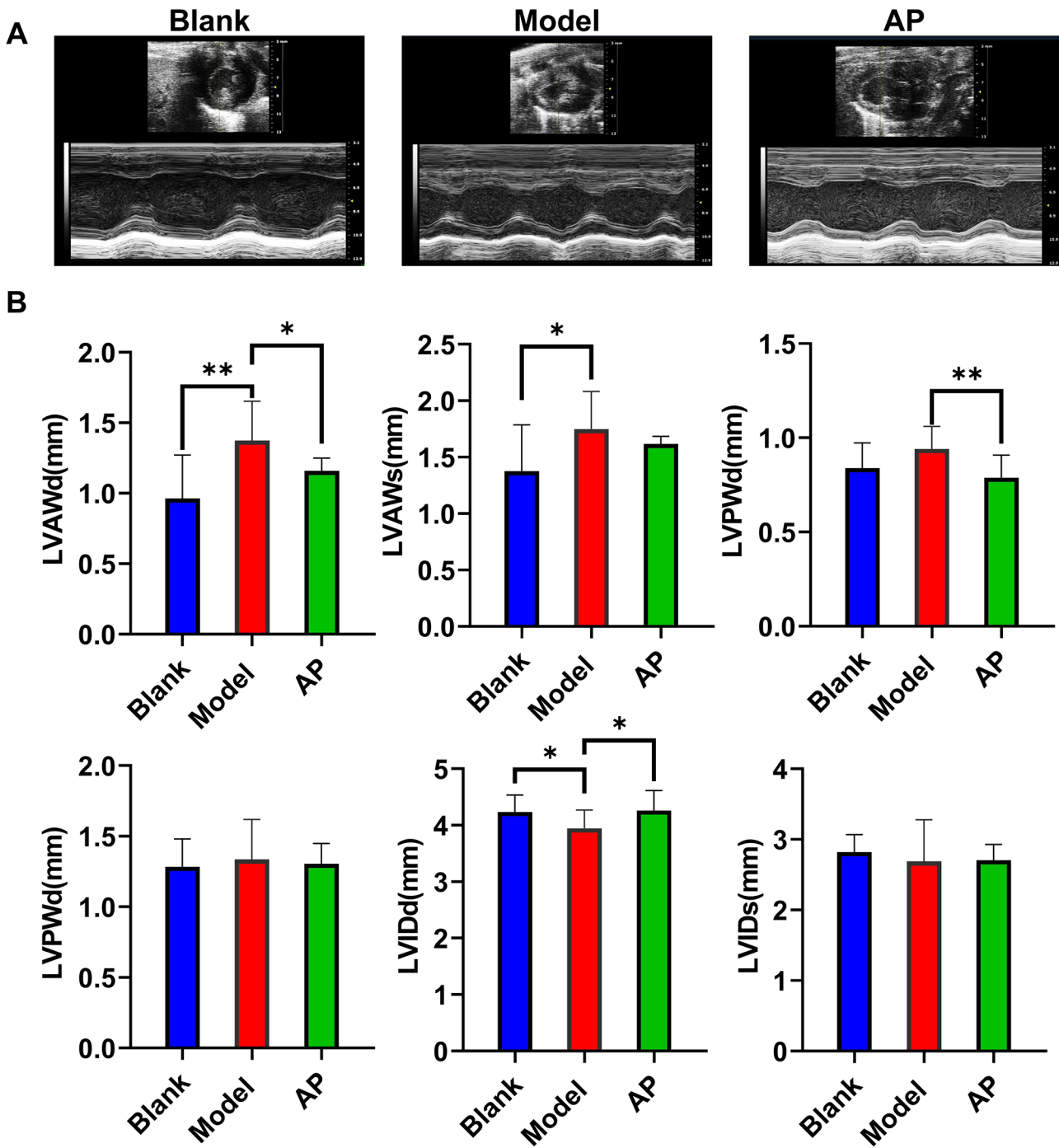
Figure 2. Echocardiographic measurements after eight weeks modeling. (A) Representative image of echocardiographic examination; (B) summarized echocardiographic measurements. Data are presented as mean value ± SD (blank $n = 11$, model $n = 9$, AP $n = 12$).
d/s: diastolic stage/systolic stage; LVAW: left ventricular anterior wall; LVPW: left ventricular posterior stage; LVID: left ventricular inner diameter.
$*P \leqslant 0.05$; $**P \leqslant 0.01$.

However, allopurinol significantly suppressed XO compare with model group (Figure 1(D)).

Echocardiographic measurements of changes in structures

The echocardiographic examination was performed after eight weeks of modeling. Through the left ventricular M-mode image, we observed that the wall thickness of the model group was increased compared with that of the blank group, and the inner diameter was correspondingly decreased due to the thickened wall. Allopurinol attenuated ventricular wall hypertrophy to some extent (Figure 2(A)). Further statistical analysis showed that the potassium oxonate and hypoxanthine co-administration treatment significantly promoted anterior wall thickening
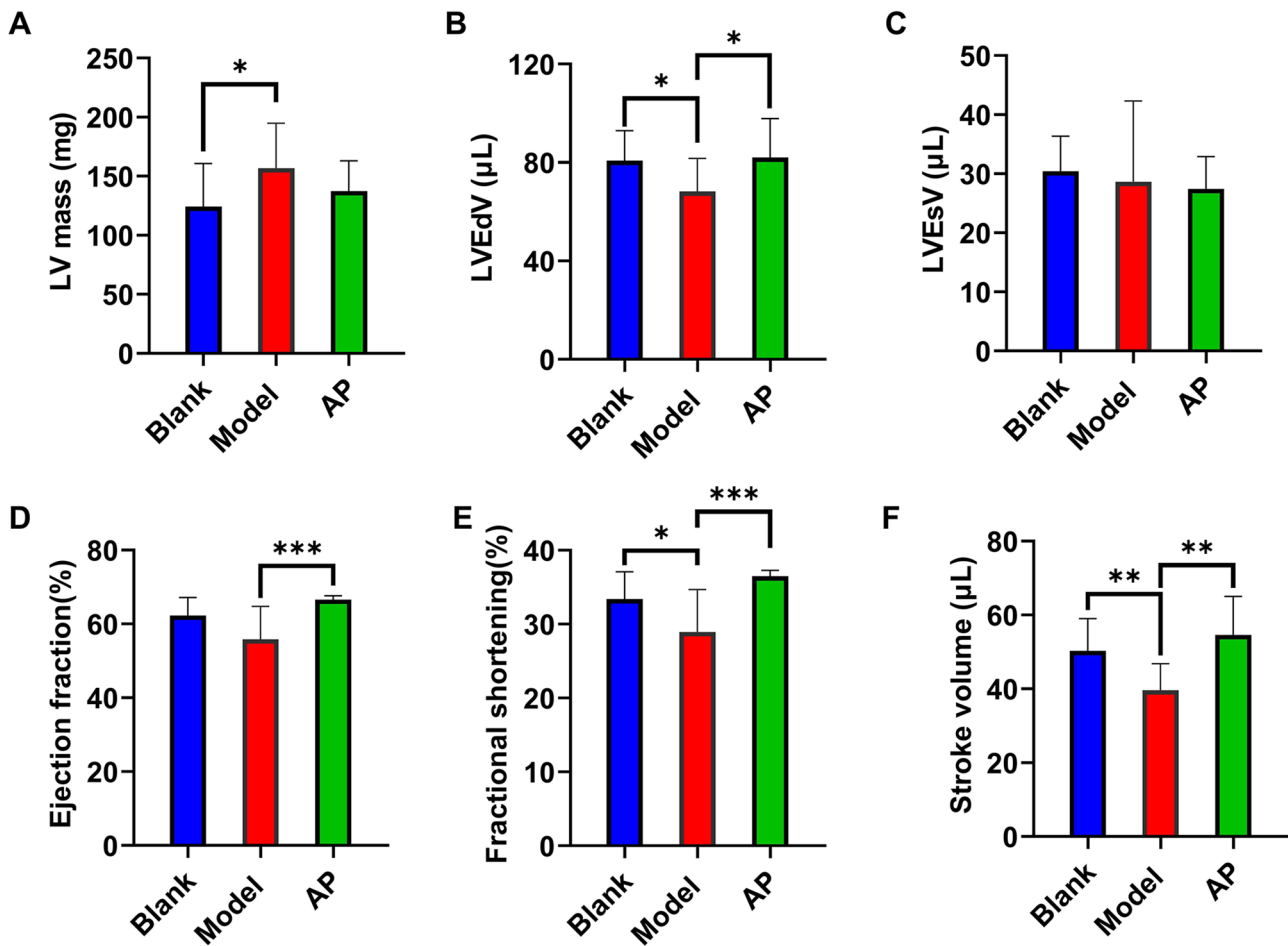
Figure 3. Cardiac functional parameters comparison among groups. (A) Left ventricular mass comparison; (B) left ventricular end-diastolic volume comparison; (C) left ventricular end-systolic volume comparison; (D) ejection fraction comparison; (E) fractional shortening comparison; (F) stroke volume comparison. Data are presented as mean value $\pm$ SD (blank $n = 11$, model $n = 9$, AP $n = 12$).
$^*P \leqslant 0.05$; $^{**}P \leqslant 0.01$; $^{***}P \leqslant 0.001$.

in both diastolic and systolic stages compared with the blank group. Although the posterior wall thickness was also increased by the model treatment compared with the blank control, the differences were not significant. The inner diameter of the model group was less than that in the blank group in the diastolic stage but not the systolic stage. Allopurinol improved the wall thickness induced by chronic HUA modeling and attenuated the decrease in the diastolic inner diameter (Figure 2(B)).

Cardiac function assessment comparison

The cardiac functional parameters can be calculated from the echocardiographic measurement values. Consistent with the cardiac hypertrophy measurements, the mass of the left ventricle was significantly increased in the model group compared with the blank group and was sensitive to allopurinol treatment (Figure 3(A)). The end volume of the model group was significantly decreased compared with that of the blank group in the diastolic stage (Figure 3(B)) but not the systolic stage (Figure 3(C)). The EF was slightly affected by the modeling treatment but did not show significant differences. This influence could be attenuated by allopurinol (Figure 3(D)). The modeling treatment significantly decreased the FS compared with the blank

treatment and could also be improved by allopurinol (Figure 3(E)). The SV was also significantly affected by the modeling treatment and improved by allopurinol (Figure 3(F)).

Heart histopathological and morphological alterations

The hearts were photographed and weighed immediately after the mice were sacrificed. From the images, we observed that the potassium oxonate and hypoxanthine co-administration method produced enlarged hearts, which was consistent with the findings in the echocardiographic parameters. Allopurinol attenuated this heart hypertrophy (Figure 4(A)). A significant difference was observed in the heart-to-body weight ratio. Allopurinol treatment slightly improved this ratio, but this trend was not statistically significant (Figure 4(B)). H&E staining showed that compared with the blank group, the model group exhibited obvious infiltration of inflammatory cells, enlarged and disorderly arranged cardiomyocytes, and dark-stained nuclei (Figure 4(C)). Masson's staining showed that compared with the blank group, the model group exhibited intercellular collagen fibrosis (Figure 4(D)). All these histopathologic changes were improved by allopurinol treatment.
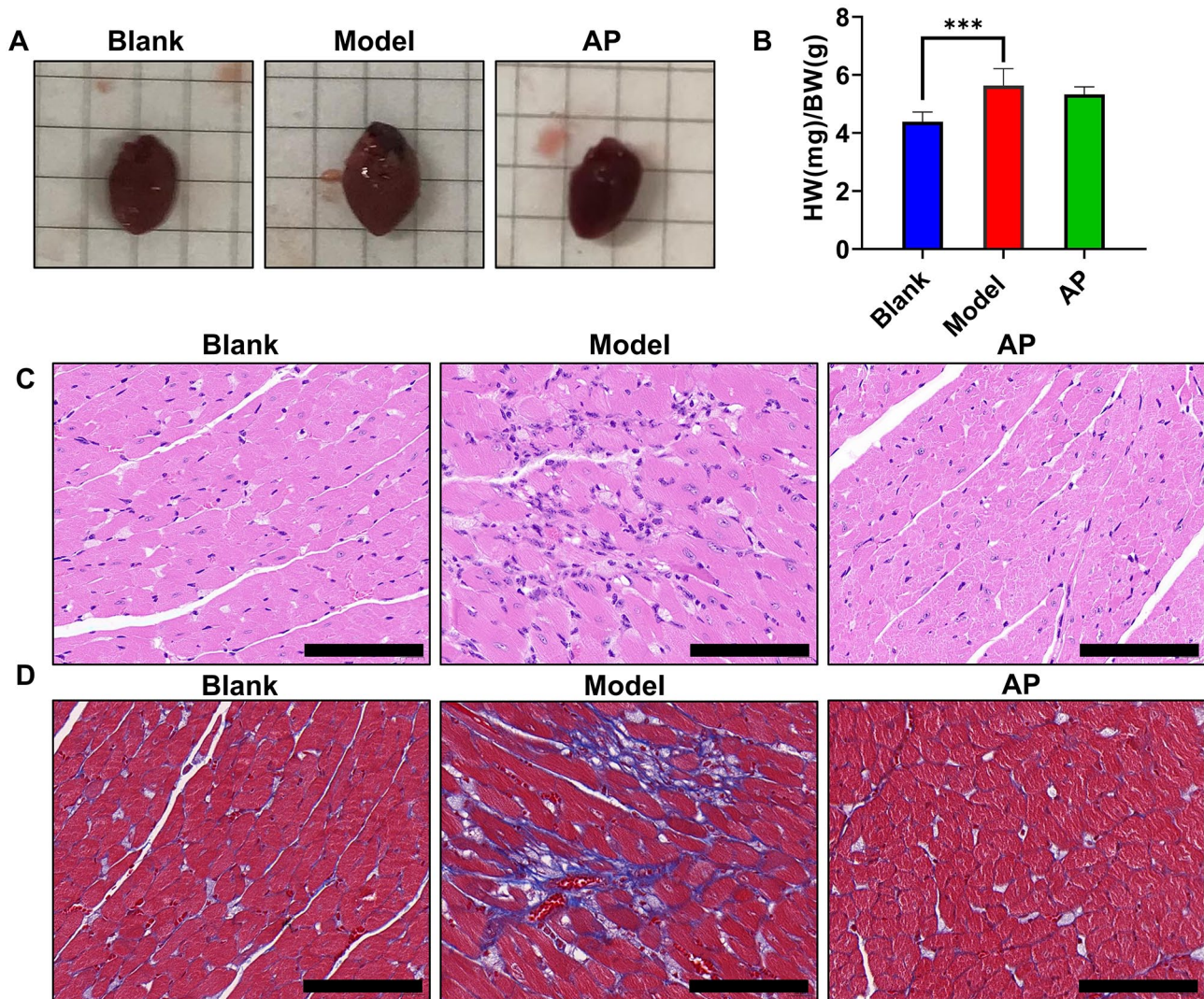
Figure 4. Morphologic and histopathologic alterations of hearts. (A) Representative image of the hearts; (B) the ratio of heart weight to body weight among the groups; (C) hematoxylin–eosin staining of left ventricular tissue under light microscopy; (D) Masson's staining of left ventricular tissue under light microscopy. Values are expressed as the mean value ± SD of determinations (blank $n = 11$, model $n = 9$, AP $n = 12$). Scale bar is 100 μM.
***$P < 0.01$.

Visualized demonstration of ventricular remodeling by the inducers

Although both intercellular synthesis and exocellular uptake are thought to be the sources of cardiomyocytic uric acid, the contribution of these two causes is still controversial. Therefore, we compared the relationship between key markers of xanthine dehydrogenase (XDH) and uric acid transport (URAT1) and markers of heart injury in both healthy donors and heart failure donors through GEO data set (GSE84796) mining. Both XDH and URAT1 correlated to some extent with the ventricular remodeling markers natriuretic peptide A (NPPA) and natriuretic peptide B (NPPB) in healthy donors but not in heart failure patients. XDH seemed to have a stronger correlation (Figure 5(A) and (B)). In the assessment of fibrosis markers, we found that URAT1 was correlated with tissue inhibitory of metaloproteinase 2 (TIMP2) and transforming growth factor beta 1 (TGFβ1), while another marker, ATP-binding cassette subfamily G member 2 (ABCG2), was negatively correlated with TGFβ1.

These findings indicate that cytoplasmic uric acid may influence cardiac fibrosis (Figure 5(C)). For heart failure prognosis, the correlation between the biomarker ST2 and URAT1 was stronger than the correlation between ST2 and XDH (Figure 5(D)). Therefore, both synthesis and transport are related to the pathological process of the heart but in different stages. We graphically summarized our modeling in Figure 5(E). Potassium oxonate inhibits UOX to prevent uric acid degradation. This therefore promotes high levels of extracellular uric acid exposure, while hypoxanthine catalysis by XO promotes cellular cytoplasm uric acid production. These two processes promote cytoplasmic uric acid accumulation and cause cardiomyocytic injury, further leading to ventricular remodeling.

Assessment of HUA-associated kidney complications

Chronic kidney disease is the most common HUA-associated complication, and this condition has been used to induce
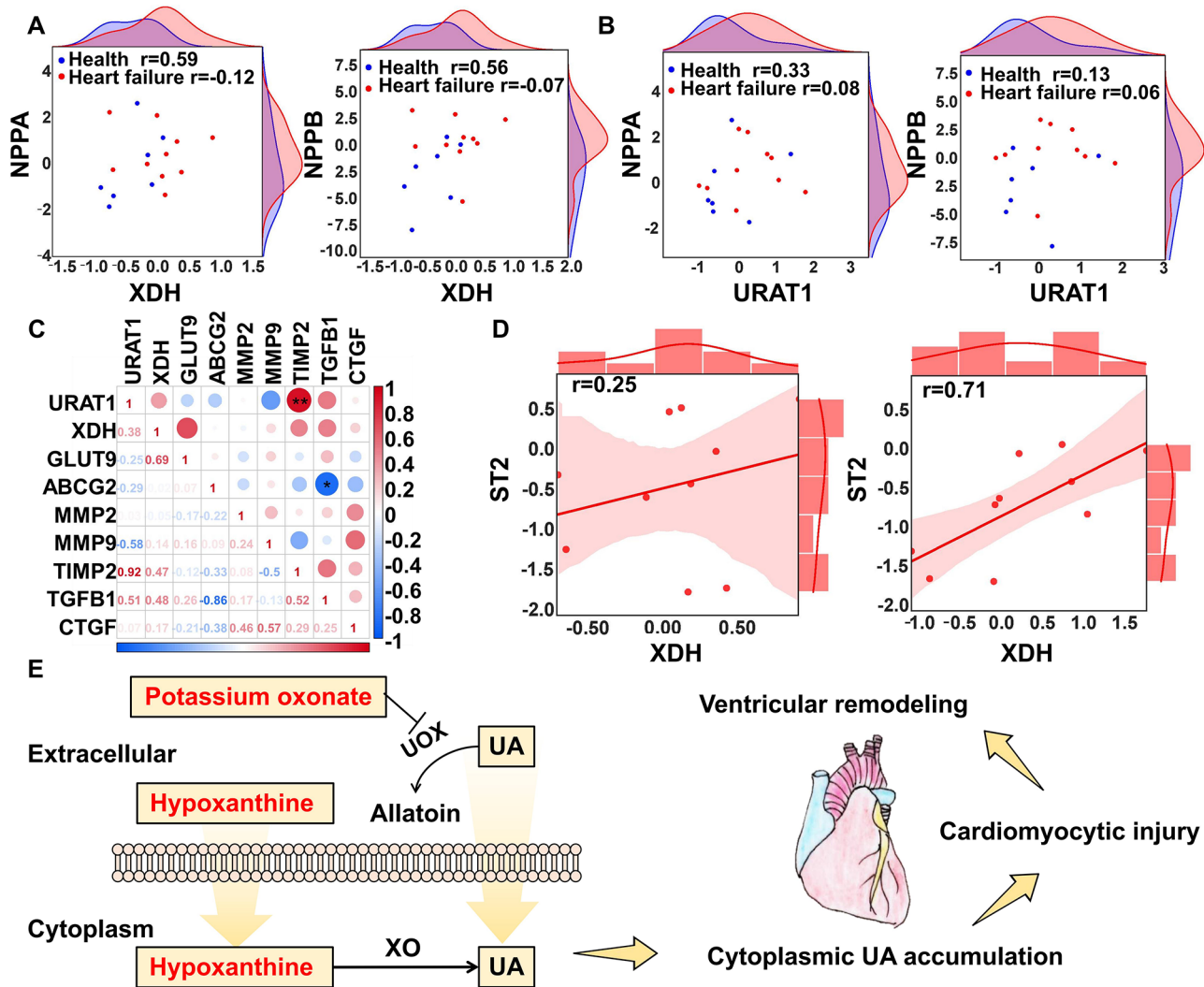
Figure 5. Visualized demonstration of the inducers. (A) Scatter points indicated relationship between XDH and NPPA and NPPB; (B) scatter points indicated relationship between URAT1 and NPPA and NPPB; (C) multiple correlation analysis between URAT1, XDH, and fibrosis markers; (D) regression curve between XDH, URAT1, and ST1 in end-heart failure patients; (E) description of the modeling rationale.

kidney injury in previous publications. We observed that compared with the blank group, the kidneys in the model group were pale and enlarged, but allopurinol attenuated this phenomenon (Figure 6(A)). A significant difference was observed in the kidney-to-body weight ratio, which is consistent with the photographic evidence (Figure 6(B)). H&E staining showed that compared with the blank group, the model group exhibited tubule dilation, infiltration of inflammatory cells, and epithelial cell vacuolation (Figure 6(C)). Masson's staining showed that compared with the blank group, the model group exhibited slight intercellular collagen fibrosis (Figure 6(D)). All these histopathologic changes were improved by allopurinol treatment.

Discussion

Most HUA-associated complication studies focus on kidney impairment or gouty arthritis development and prevention. Compared with kidney and joint injury research, research on HUA-associated cardiovascular complications is still in its infancy. In 2014, a large retrospective study revealed that every 1 mg/dL increase in serum uric acid was associated with a 19% increase in the incidence of heart failure and a 4% increase in the all-cause mortality risk.[3] The cut-off uric acid value is 5.6 mg/dL in most cardiovascular mortality, while 5.27 mg/dL in women and 5.49 mg/dL in men with myocardial infarction, 4.87 mg/dL in fatal heart failure.[14] However, the option of choosing urate-lowering agents is limited, and the influence of current common urate-lowering agents on cardiovascular is controversial and unsatisfactory.[15–18] Therefore, more *in vivo* mechanism investigation and assessment of therapeutic treatments for HUA-associated cardiovascular disease are essential. A valid model will be useful for future exploration.

As mentioned above, a proven valid heart injury animal model of HUA would be beneficial to future research. The chemically induced method is a mainstream modeling strategy due to its low cost. The common inducers include potassium oxonate, hypoxanthine, yeast extract, adenine, ethambutol, nicotinic acid, and fructose.[19,20] Currently, several studies have also used different models to promote HUA-associated cardiomyocytic injury *in vivo*. Guanghong
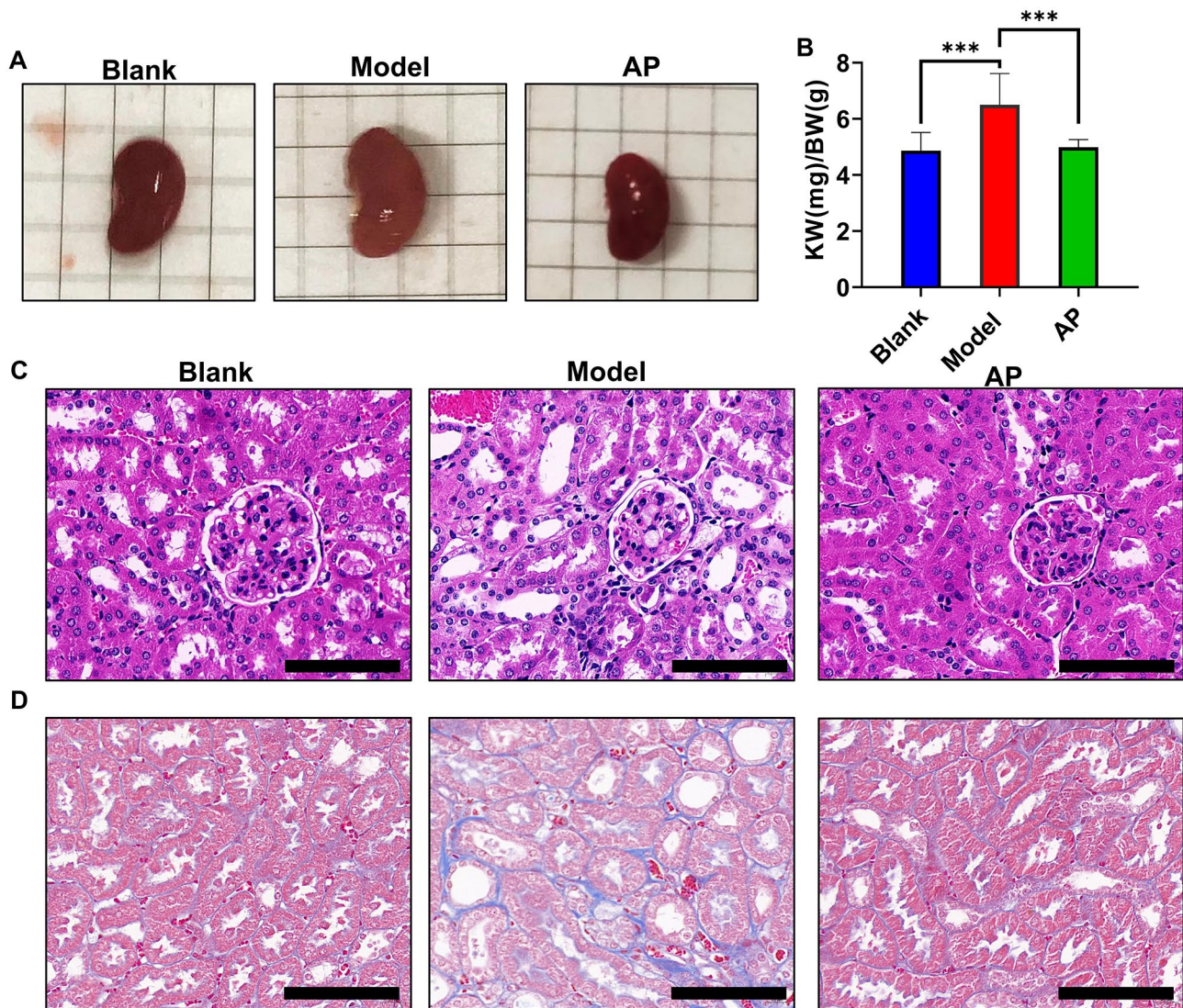
Figure 6. Morphologic and histopathologic alterations of kidneys. (A) Representative image of the kidneys; (B) the ratio of kidney weight to body weight among the groups; (C) hematoxylin–eosin staining of kidney under light microscopy; (D) Masson's staining of kidney under light microscopy. Values are expressed as the mean value $\pm$ SD of determinations (blank $n=11$, model $n=9$, AP $n=12$). Scale bar is 100 μM.
***$P < 0.001$.

Jia *et al*. used a Western diet formula consisting of a high-fat content (46%) and a high carbohydrate component from sucrose (17.5) and high-fructose corn syrup (17.5%). This Western diet was fed to male C57BL6/J mice for 16 weeks. The plasma uric acid concentration of the model group was 0.68 ± 0.07 mg/dL, which was higher than that of the blank group (0.50 ± 0.06 mg/dL). At the termination of this study, the model group showed cardiomyocyte hypertrophy, myocardial oxidative stress, interstitial fibrosis, and impaired diastolic relaxation.[10] Meilin Yan *et al*. used the oxonic acid gavage method to treat SD rats for 16 weeks. The serum uric acid of the model group was 2.96 ± 0.32 mg/dL, and in the blank group, it was 1.17 ± 0.14 mg/dL. They ultimately observed increased left ventricular end-diastolic pressure, cardiomyocytic apoptosis, and interstitial fibrosis in the model group.[11] Hailong Zhang *et al*. administered adenine and ethambutol for 33 days to induce HUA in the Wistar rats. They found that the serum uric acid level was approximately 25 mg/dL in the model group, and in the blank group, it

was approximately 5 mg/dL. Furthermore, the model group showed myocardial inflammation and damage.[21] HUA is as serum uric acid ≥7 mg/dL (420 mmol/L) in men or ≥6 mg/dL (360 mmol/L) in women.[22] Throughout the duration of our experiment, the plasma uric acid concentration of the model group remained in the range of 10~20 mg/dL, fitting the clinical diagnostic criteria. This was significantly higher than that in the blank control group. Furthermore, these levels were decreased by the urate-lowering agent allopurinol. This suitable concentration is an advancement compared with others.

In clinical data, the correlation between cardiovascular issues and HUA in the healthy population is not significant.[23] However, in the condition of accompanying with other basic diseases such as hypertension, atrial fibrillation, and type 2 diabetes, HUA accelerates cardiac hypertrophy with no obvious EF change.[24–27] Consistently, our heart weight data also showed an enlarged heart with limited parameter impairment. Echocardiography examination indicated that

the modeling method mainly influenced the ventricular end in the diastolic stage but not in the systolic stage. Both cardiac function and histological changes can be improved by allopurinol. This result is consistent with previously published results.[10] However, we noticed that the anterior wall thickness is more sensitive to the modeling inducers compared with the posterior portion. More effort is needed to explain this phenomenon.

The pathological basis of chronic heart failure incidence and development is a vicious cycle of heart remodeling.[28] Currently, there are two distinct mechanisms still in controversy about HUA-associated cardiovascular diseases. Some researchers believe HUA-associated cardiovascular diseases are related with the reactive oxygen species produced by XO-mediated purine metabolism,[14] while the others believe extracellular soluble uric acid is a direct trigger of cardiomyocytes injury, and subsequently promotes cardiac pathological change.[21] Therefore, we performed a bioinformatic analysis to explore the correlation ship of ventricular markers with purine metabolism–related XDH and uric acid membrane transportation–related URAT1. Our bioinformatic analysis showed that purine metabolism may make substantial contributions to the health condition of remodeling, and uric acid uptake may play a more important role in the condition of heart failure. Therefore, a model with increased purine metabolism and increased extracellular uric acid is benefit to investigate HUA-associated ventricular remodeling. Of the two inducers, potassium oxonate is targeted to increase extracellular uric acid concentrations, and hypoxanthine is targeted to increase the purine metabolic source. This finding fits the mechanism of cardiomyocytic injury.

Chronic kidney injury is the most commonly reported HUA-associated complication in clinical epidemiological research.[29,30] Previous publications also showed that the co-administration of potassium oxonate and hypoxanthine promoted kidney injury when accompanied by modeling.[31,32] After eight weeks of modeling, we also observed kidney injury to some extent, which is consistent with previous reports. Chronic kidney disease is also known as a promoter of cardiovascular diseases. Some risk factor of ventricular remodeling is related to the cardiorenal syndrome.[33] The majority of researches believe that kidney injury leads to renin–angiotensin system activation followed by angiotensin II increasing, which triggers the increase in cardiac afterload and causes cardiac adaptive responsible hypertrophy.[33,34]

Some shortcomings of this study should be mentioned. The ventricular remodeling is a continuous process. In the early stage, it shows diastolic dysfunction and accompany with ventricular wall hypertrophy. Under the condition that the risk factors persist, the late stage of ventricular remodeling shows systolic dysfunction and accompany with ventricular wall thinning.[35–37] Some researchers proposed that uric acid may act on heart in an early unstable stage of the disease; in the stable stages, other factors may overshadow its effects.[38] However, we did not monitor the weekly changes in cardiac function and heart hemodynamically. And also did not prolong the modeling period to observe the continuous consequence.

This study systematically assessed the ventricular remodeling–inducing effect of a chronic HUA model induced by potassium oxonate and hypoxanthine. This study provides useful information for further investigation and the therapeutic treatment evaluation of future HUA-associated heart injury mechanisms.

AUTHORS' CONTRIBUTIONS

CL, YY, and JP conceived and designed the study. CL and QZ prepared the inducers and medicine. CL and YL were in charge of daily modeling and drug treatment. QZ, JL, TW, YJ, QH, CY, and LZ were in charge of animal feeding and environmental management, weight and diet records. WZ and HL helped record data to spreadsheets. CL and YY performed animal anesthetics and cardiac ultrasound examination. All authors participated in the activity of mice sacrifice and tissue harvest. CL, YY, and QZ performed plasma and tissue examination. YY performed the bioinformatic analysis. CL, YY, and JP wrote the manuscript.

DECLARATION OF CONFLICTING INTERESTS

The author(s) declared no potential conflicts of interest with respect to the research, authorship, and/or publication of this article.

ORCID ID

Jianxin Pang 🆔 https://orcid.org/0000-0002-0053-2723

REFERENCES

1. Gromadziński L, Januszko-Giergielewicz B, Pruszczyk P. Hyperuricemia is an independent predictive factor for left ventricular diastolic dysfunction in patients with chronic kidney disease. *Adv Clin Exp Med* 2015;**24**:47–54

2. Yu S, Yang H, Guo X, Zheng L, Sun Y. Hyperuricemia is independently associated with left ventricular hypertrophy in post-menopausal women but not in pre-menopausal women in rural Northeast China. *Gynecol Endocrinol* 2015;**31**:736–41

3. Huang H, Huang B, Li Y, Huang Y, Li J, Yao H, Jing X, Chen J, Wang J. Uric acid and risk of heart failure: a systematic review and meta-analysis. *Eur J Heart Fail* 2014;**16**:15–24

4. Tamariz L, Hernandez F, Bush A, Palacio A, Hare JM. Association between serum uric acid and atrial fibrillation: a systematic review and meta-analysis. *Heart Rhythm* 2014;**11**:1102–8

5. Borghi C, Domienik-Karłowicz J, Tykarski A, Widecka K, Filipiak KJ, Jaguszewski MJ, Narkiewicz K, Mancia G. Expert consensus for the diagnosis and treatment of patient with hyperuricemia and high cardiovascular risk: 2021 update. *Cardiol J* 2021;**28**:1–14

6. Wu XW, Muzny DM, Lee CC, Caskey CT. Two independent mutational events in the loss of urate oxidase during hominoid evolution. *J Mol Evol* 1992;**34**:78–84

7. Bannasch D, Safra N, Young A, Karmi N, Schaible RS, Ling GV. Mutations in the SLC2A9 gene cause hyperuricosuria and hyperuricemia in the dog. *Plos Genet* 2008;**4**:e1000246

8. Wu X, Wakamiya M, Vaishnav S, Geske R, Montgomery C Jr, Jones P, Bradley A, Caskey CT. Hyperuricemia and urate nephropathy in urate oxidase-deficient mice. *Proc Natl Acad Sci U S A* 1994;**91**:742–6

9. Lu J, Hou X, Yuan X, Cui L, Liu Z, Li X, Ma L, Cheng X, Xin Y, Wang C, Zhang K, Wang X, Ren W, Sun R, Jia Z, Tian Z, Mi QS, Li C. Knockout

of the urate oxidase gene provides a stable mouse model of hyperuri-cemia associated with metabolic disorders. *Kidney Int* 2018;**93**:69–80

10. Jia G, Habibi J, Bostick BP, Ma L, DeMarco VG, Aroor AR, Hayden MR, Whaley-Connell AT, Sowers JR. Uric acid promotes left ven-tricular diastolic dysfunction in mice fed a Western diet. *Hypertension* 2015;**65**:531–9

11. Yan M, Chen K, He L, Li S, Huang D, Li J. Uric acid induces cardiomyo-cyte apoptosis via activation of Calpain-1 and endoplasmic reticulum stress. *Cell Physiol Biochem* 2018;**45**:2122–35

12. Mangoff SC, Milner JA. Oxonate-induced hyperuricemia and orotic aciduria in mice. *Proc Soc Exp Biol Med* 1978;**157**:110–5

13. Schmidt HM, Kelley EE, Straub AC. The impact of xanthine oxidase (XO) on hemolytic diseases. *Redox Biol* 2019;**21**:101072

14. Maloberti A, Biolcati M, Ruzzenenti G, Giani V, Leidi F, Monticelli M, Algeri M, Scarpellini S, Nava S, Soriano F, Oreglia J, Sacco A, Morici N, Oliva F, Piani F, Borghi C, Giannattasio C. The role of uric acid in acute and chronic coronary syndromes. *J Clin Med* 2021;**10**:4750

15. White WB, Saag KG, Becker MA, Borer JS, Gorelick PB, Whelton A, Hunt B, Castillo M, Gunawardhana L, CARES Investigators. Cardio-vascular safety of febuxostat or allopurinol in patients with gout. *N Engl J Med* 2018;**378**:1200–10

16. Mackenzie IS, Ford I, Nuki G, Hallas J, Hawkey CJ, Webster J, Ralston SH, Walters M, Robertson M, De Caterina R, Findlay E, Perez-Ruiz F, McMurray J, MacDonald TM, FAST Study Group. Long-term cardio-vascular safety of febuxostat compared with allopurinol in patients with gout (FAST): a multicentre, prospective, randomised, open-label, non-inferiority trial. *Lancet* 2020;**396**:1745–57

17. Ogino K, Kato M, Furuse Y, Kinugasa Y, Ishida K, Osaki S, Kinugawa T, Igawa O, Hisatome I, Shigemasa C, Anker SD, Doehner W. Uric acid-lowering treatment with benzbromarone in patients with heart failure: a double-blind placebo-controlled crossover preliminary study. *Circ Heart Fail* 2010;**3**:73–81

18. Kang EH, Park EH, Shin A, Song JS, Kim SC. Cardiovascular risk associated with allopurinol vs. benzbromarone in patients with gout. *Eur Heart J* 2021;**42**:4578–88

19. Zhu Y, Peng X, Ling G. An update on the animal models in hyper-uricaemia research. *Clin Exp Rheumatol* 2017;**35**:860–4

20. Lu J, Dalbeth N, Yin H, Li C, Merriman TR, Wei WH. Mouse models for human hyperuricaemia: a critical review. *Nat Rev Rheumatol* 2019;**15**:413–26

21. Zhang H, Ma Y, Cao R, Wang G, Li S, Cao Y, Zhang H, Liu M, Liu G, Zhang J, Li S, Wang Y, Ma Y. Soluble uric acid induces myocardial damage through activating the NLRP3 inflammasome. *J Cell Mol Med* 2020;**24**:8849–61

22. Chen Y, Zhang N, Sun G, Guo X, Yu S, Yang H, Zheng L, Sun Y. Metabolically healthy obesity also has risk for hyperuricemia among Chinese general population: a cross-sectional study. *Obes Res Clin Pract* 2016;**10**:S84–95

23. Maloberti A, Qualliu E, Occhi L, Sun J, Grasso E, Tognola C, Tavecchia G, Cartella I, Milani M, Vallerio P, Signorini S, Brambilla P, Casati M, Bombelli M, Grassi G, Giannattasio C. Hyperuricemia prevalence in healthy subjects and its relationship with cardiovascular target organ damage. *Nutr Metab Cardiovasc Dis* 2021;**31**:178–85

24. Liang WY, Liu WW, Liu ML, Xiang W, Feng XR, Huang B, Chen XH, Sun YS. Serum uric acid level and left ventricular hypertrophy in elderly male patients with nonvalvular atrial fibrillation. *Nutr Metab Cardiovasc Dis* 2016;**26**:575–80

25. Wang Q, Tan K, Xia H, Gao Y. The further negative effect of hyperuri-cemia on left ventricular structure and function in patients with Type 2 diabetes mellitus: a transthoracic 3D speckle tracking imaging study. *Metab Syndr Relat Disord* 2019;**17**:436–43

26. Adewuya OA, Ajayi EA, Adebayo RA, Ojo OE, Olaoye OB. Serum uric acid and left ventricular hypertrophy in hypertensive patients in Ado-Ekiti. *Pan Afr Med J* 2020;**36**:190

27. Maloberti A, Maggioni S, Occhi L, Triglione N, Panzeri F, Nava S, Signorini S, Falbo R, Casati M, Grassi G, Giannattasio C. Sex-related relationships between uric acid and target organ damage in hyperten-sion. *J Clin Hypertens (Greenwich)* 2018;**20**:193–200

28. Weber KT, Brilla CG. Structural basis for pathologic left ventricular hypertrophy. *Clin Cardiol* 1993;**16**:II10–4

29. Nashar K, Fried LF. Hyperuricemia and the progression of chronic kidney disease: is uric acid a marker or an independent risk factor. *Adv Chronic Kidney Dis* 2012;**19**:386–91

30. Oh TR, Choi HS, Kim CS, Bae EH, Ma SK, Sung SA, Kim YS, Oh KH, Ahn C, Kim SW. Hyperuricemia has increased the risk of progression of chronic kidney disease: propensity score matching analysis from the KNOW-CKD study. *Sci Rep* 2019;**9**:6681

31. Lu YH, Chang YP, Li T, Han F, Li CJ, Li XY, Xue M, Cheng Y, Meng ZY, Han Z, Sun B, Chen LM. Empagliflozin attenuates hyperuricemia by upregulation of ABCG2 via AMPK/AKT/CREB signaling pathway in type 2 diabetic mice. *Int J Biol Sci* 2020;**16**:529–42

32. Xu L, Lin G, Yu Q, Li Q, Mai L, Cheng J, Xie J, Liu Y, Su Z, Li Y. Anti-hyperuricemic and nephroprotective effects of dihydroberberine in potassium oxonate- and hypoxanthine-induced hyperuricemic mice. *Front Pharmacol* 2021;**12**:645879

33. Hatamizadeh P, Fonarow GC, Budoff MJ, Darabian S, Kovesdy CP, Kalantar-Zadeh K. Cardiorenal syndrome: pathophysiology and potential targets for clinical management. *Nat Rev Nephrol* 2013;**9**:99–111

34. Ham O, Jin W, Lei L, Huang HH, Tsuji K, Huang M, Roh J, Rosenzweig A, Lu H. Pathological cardiac remodeling occurs early in CKD mice from unilateral urinary obstruction, and is attenuated by Enalapril. *Sci Rep* 2018;**8**:16087

35. Palmieri V, Wachtell K, Gerdts E, Bella JN, Papademetriou V, Tuxen C, Nieminen MS, Dahlöf B, de Simone G, Devereux RB. Left ventricular function and hemodynamic features of inappropriate left ventricular hypertrophy in patients with systemic hypertension: the LIFE study. *Am Heart J* 2001;**141**:784–91

36. Meerson FZ. On the mechanism of compensatory hyperfunction and insufficiency of the heart. *Cor Vasa* 1961;**3**:161–77

37. Frey N, Katus HA, Olson EN, Hill JA. Hypertrophy of the heart: a new therapeutic target. *Circulation* 2004;**109**:1580–9

38. Maloberti A, Bossi I, Tassistro E, Rebora P, Racioppi A, Nava S, Soriano F, Piccaluga E, Piccalò G, Oreglia J, Vallerio P, Pirola R, De Chiara B, Oliva F, Moreo A, Valsecchi MG, Giannattasio C. Uric acid in chronic coronary syndromes: relationship with coronary artery disease severity and left ventricular diastolic parameter. *Nutr Metab Cardiovasc Dis* 2021;**31**:1501–8